SCIREA Journal of Materials Science

http://www.scirea.org/journal/Materials

November 11, 2016

Volume 1, Issue1, October 2016

Spotlight on the Nano-Structural Features of Mn-Doped-Aurivillius Phase For Catalysis Applications An AFM-Studies

Khaled M. Elsabawy[a,b,*]

a: Materials Science Unit, Chemistry Department,Faculty of Science,Tanta University- Tanta-EGYPT

b: Materials Science Unit ,Chemistry Department,Faculty of Science,,Taif University,Taif, Saudi Arabia

*Corresponding author: Prof.Dr. Khaled M. Elsabawy

E-mail address: ksabawy@yahoo.com , khaledelsabawy@yahoo.com

Abstract

The aurivillius phase of optimum Mn-doped with chemical formula $Bi_2SrV_{1.9}Mn_{0.1}O_9$ was carefully prepared by solid state reaction technique and ceramics procedures. The analysis of X-ray confirmed the formation of single aurivillus layered perovskite structure. The sample well characterized and then forwarded to both of SEM and AFM-investigations to predict nano-structural feature and huge surface area topology which qualifies this family of aurivillus with high oxygen content (O=9) to be active surface material in heterogeneous catalysis processes.

Keywords: Manganese; Vanadium sites; Perovskite; Ceramic; X-ray; AFM; SEM

I - Introduction:

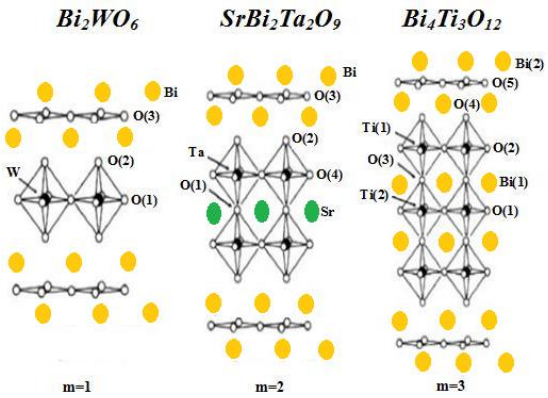

Several bismuth layered aurivillius perovskites such as strontium bismuth niobate [SBN] tungestate or tantalate with oxygen content equal ~9 212 or 122-phase [1] and strontium bismuth tantalate [SBT] [2] have been shown to exhibit much elongated fatigue durability and are capable of withstanding 10^{12} erase and rewrite operations. It's found that the substitution of niobium with vanadium in $SrBi_2Nb_2O_9$ leads to enhancement of ferroelectric properties together with a lowered processing temperature [3-5]. It has recently been reported that there occurs ($BiFeO_3$) doped Sr Bi Nb [6]. Most of the work of the layered perovskite Sr Bi oxides reported on the improvement of the dielectric and ferroelectric properties are based on A-site substitution [7-9]. For example the replacement of Sr^{2+} ions by a smaller cations Ca^{2+} result in an increase in its dielectric content and Curies temperature Tc [10].

In spite of there is no any extensive study on dielectric properties of layered perovskite, through B-site, The effect of tungsten substitutions for tantalum on the structural, dielectric and impedance properties, of $SrBi_2Ta_2O_9$ ferroelectric ceramics[11].

We attempted to synthesize for layered hexagonal $(Sr_{1-x}La_x)$ MnO_3ceramics. However, we couldn't obtain the single phased $(Sr_{1-x}La_x)$ MnO_3. It was difficult to accommodate the Mn^{3+} ion with large ionic radius to the lattice because the ionic radius of the La^{3+} ion was smaller than that of the Sr^{2+} ions [12]. The lattice constants (a and c) for layered hexagonal $(Sr_{1-x}Ba_x)MnO_3$ $(0 \leq x \leq 0.5)$ increase linearly with the increase of Ba content [13]. It's well known that the addition of 3d transition metals e.g. Mn, Fe, Cr and Cu improves the dielectric properties of bismuth strontium titanate and that Mn is the most effective among them, Mn ions are belived to substitute Ti and act as acceptors [14-16]. Recently, it was found by Liu et al. that Ca and Mn co-doping effects on the structure and dielectric properties of sol-gel derived BST ceramics [17].

It is well known that Mn doped Barium Strontium Titanate was unable to change the perovskite crystallizing structure in BST materials, also, the scanning electron micrograph revealed that the crystalline grains become larger with increasing the content of Mn doping when Mn is below 1.5 % and the grains size decreased after the Mn content exceeded 1.5 %. Two types effects were founding the Mn-doped BST-MT composite ceramics. One is the doping effects when Mn was below 1.5 % where, Mn acts as an acceptor to replace Ti at the B-site perovskite ABO_3 structure. The other was composite effect when Mn contents are above 1.5 % [18]. Perovskite –type oxide such as $CaMnO_3$, have two way for substitution, the first at Ca site as reported in [19] and the second is doping Mn-site with the cation having valency higher than four. Pentavalent ions such as Nb, Ta, and Ru can be considered for Mn-site doping. Among Nb, Ta and Ru, we preferred Ru because Ru^{5+} has 4d electrons while Nb^{5+} and Ta^{5+} have none [20].

The partial B-site acceptor substitution of the $(K_{0.45}Bi_{0.55})$ $Bi_4Ti_4O_{15}$ (KBTi) thin films with M = Mn^{2+}, Fe^{3+}, and Ni^{2+} to form non-lanthanide $(K_{0.45}Bi_{0.55})$ Bi $(Ti_{0.38}M_{0.2})$ O_{15}. Ti-containing perovskites have tendency of undergoing the $Ti^{4+} \longrightarrow Ti^{3+}$ transition. The doner substituted $(K_{0.45}Bi_{0.55})$ at the A-site instead of the even-distributed $(K_{0.5}Bi_{0.5})$ for KBTi films can firstly compensate for the charge unbalance due to the $Ti^{4+} \longrightarrow Ti^{3+}$ transitions and secondly provide the opportunity for the acceptor substitution at B-site with fewer oxygen vacancies [21].

The essential goal of the present article is to focus on the nano-structural features and surface area topology of 212 Bi-Sr-V-O regime to play as active surface catalyst on the industrial applications .

II - Experimental:

The optimum Mn- doped aurivillus sample with x= 0.1 mole was selected from previously work with the general formula $Bi_2SrV_{1.9}Mn_{0.1}O_9$ was prepared by conventional solid state reaction route and sintering procedure using (physical method) the appropriate amounts of $Bi_2(CO_3)_3$, $SrCO_3$, $(NH_4)_2VO_3$ and MnO (each purity >99%).The particles size of MnO applied as dopant was ranged in between 60-90 nm. The mixture was ground in an agate mortar for one hour. Then the finely ground powder was subjected to firing at 800 ^oC for 12 hours, reground and finally pressed into pellets with thickness 0.2 cm, diameter 1.2 cm and

Sintered at 840 ^{o}C for 20 hours. Then the furnace is cooled slowly down to room temperature. Finally the materials are kept in vacuum desiccator over silica gel dryer.

II.I- Structural Measurements:

II.I.A. X-Ray diffraction (XRD):

The X-ray diffraction measurements (XRD) were carried out at room temperature on the fine ground $Bi_2SrV_{1.9}Mn_{0.1}O_9$ in the range (2θ =10-70^{o}) using Cu-Kα radiation source and a computerized [Bruker Axs-D8 advance] X-ray diffractometer with two theta scan technique.

II.I.B. Solid infrared absorption spectral measurements:

The IR absorption spectra of the prepared samples were recorded using " Nexus 670 FT IR spectrometer in the range 500-2500 cm^{-1} using pure KBr matrix".

II.I.C. AFM and Scanning Electron – Microscopy:

Scanning electron microscope (SEM) measurements were carried out using small pieces of prepared samples on different sectors to be the actual molar ratios by using "TXA-840,JEOL-Japan" attached to XL30 apparatus with EDX unit, accelerant voltage 30kv, magnification 10x up to 500.000x and resolution 3. nm.

Atomic force microscopy (AFM): High-resolution Atomic Force microscopy (AFM) is used for testing morphological features and topological map (Veeco-di Innova Model-2009-AFM-USA).The applied mode was tapping non-contacting mode. For accurate mapping of the surface topology AFM-raw data were forwarded to the Origin-Lab version 6-USA program to visualize more accurate three dimension surface of the sample under investigation Mn-optimally doped aurivillus phase . This process is new trend to get high resolution 3D-mapped surface for very small area ~ 0.1x0.1 μm^2.

III - Results & Discussion:

III.I-Phase Identification:

III.I.A X-ray Diffraction:

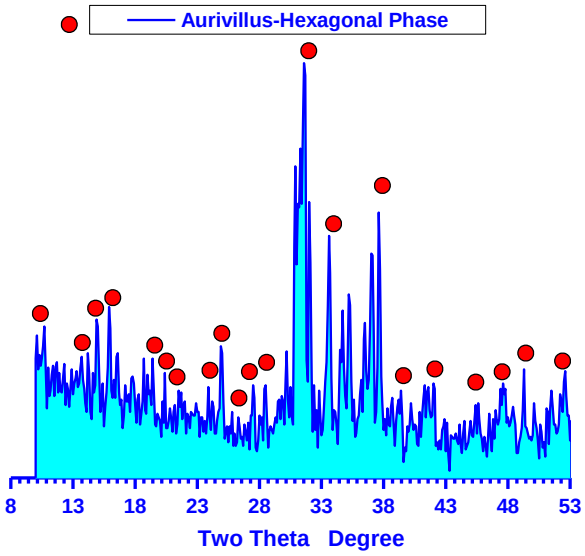

Fig (1): XRD patterns recorded for optimum Mn-doped sample $Bi_2SrV_{1.9}Mn_{0.1}O_9$.

Fig.(1) displays the X-ray diffraction patterns of Mn-doped samples having the general formula $Bi_2SrV_{2-x}Mn_xO_9$, where x = 0.1 mole.

Analysis of the corresponding 2θ values and the interplanars spacings d (A^o) by using computerized program proved that the compound mainly belongs to distorted aurivillius structure type with hexagonal crystal form, that expressed by assigned peaks. The unit cell dimensions were calculated using parameter of the most intense X-ray reflection peaks and found to be a = b = 5.7804 A^o and c = 7.104 A^o for Mn-212 Bi-Sr-V-O regime.

The substitution of Mn for V^{5+} would induce B-site cation vacancies in the aurivillius layer structure which leads to an increasing of internal stress for the shrinkage of unit cell volume. It's observed that the single phase layered auivillius structure is obtained in the range $0 \leq x \leq 0.6$ since the intensity of the peaks increases as the Mn doping increases. The lattice parameter c shows an increasing as the x-values increase, due to the stress inside the lattice which leads to increase the shrinkage of lattice.

III.I.B. Solid infrared absorption spectral measurements:

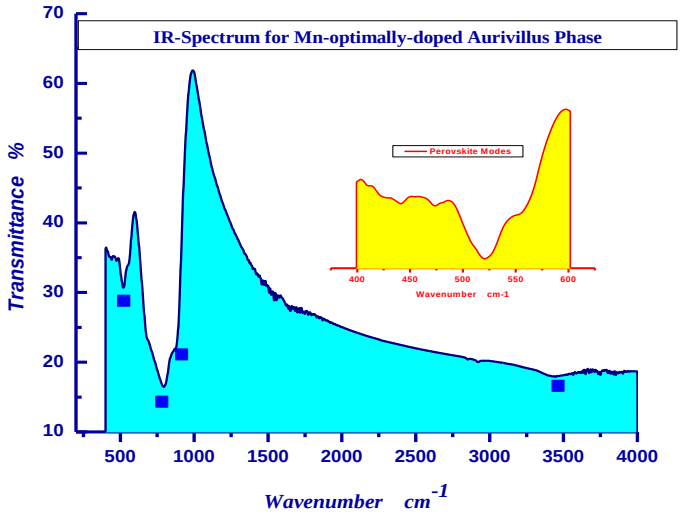

Fig.2: IR absorption spectra recorded for Mn-optimally-doped aurivillius phase .

The IR absorption spectra of Mn- 212BiSrV sample was carried out at room temperature in the IR range of 400 – 600 cm^{-1} as shown in Fig.(2) yellow figure. The system $212BiSrVO_{9}\pm\delta$ is mainly belongs to deficient perovskite structure and extra oxygen atom $O_{9}\pm\delta$. Oxygen nine makes the structure to be distorted perovskite, so the vibrational modes of IR spectra of perovskite are closely appear.

In the system under investigation, the V site in the ABO_3 crystal structure is being modified. Further, it's also well accepted that the displacement of V ions from its center caused ferroelectricity in these materials. Therefore an investigation of the infrared absorption is expected to reveal valuable information about the modification caused in the interatomic forces between V and O ions with the substitutions.

The IR absorption bands in the range of 400-600 cm^{-1} are assigned to the stretching and bending modes of vibration of Bi-O, Sr-O, V-O / Mn-O and Bi-O-V, Bi-O-Sr, respectively [38]. The band around 800 cm^{-1} is reported to be dominated by the motion of oxygen sub-lattice [22].

III.I.C. 3D-AFM investigations & Microstructural properties (SEM):

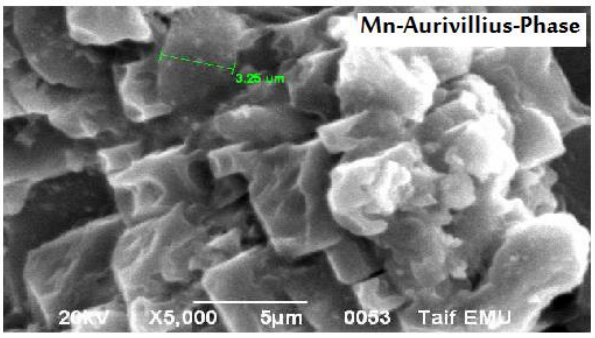

Fig.3a: SE-micrograph recorded for Mn-doped 212-aurivillius-phase .

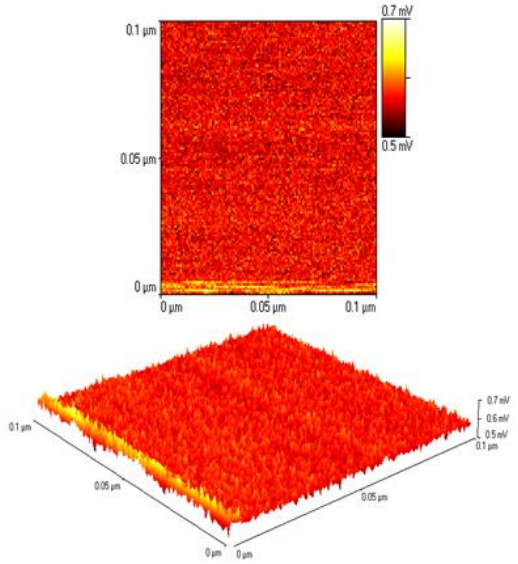

Fig.3b: 2&3D-AFM Nano-graph recorded for Mn-doped 212-aurivillius-phase .

Fig.(3_a) displays the SEM-micrographs captured for the synthesized material Mn-optimally doped 212-BiSrV . As it is clear the grain size of Mn- 212BiSrV is found to be in between 0.56-2.5 µm. The presence of bismuth leads to attraction between the grains with each other and porous structure appeared between the grains due to bismuth evaporation (Fig. 3_a).

The grain size increased drastically with increase of Mn addition from 0.1 to 0.3 moles as reported in [23] and found to be in between 2.49-2.6 µm respectively. The ionic radius of Mn^{2+} is 67 pm which is close to the ionic radius of V^{5+} 58 pm, Mn will replace V at the B-site of the perovskite ABO_3 structure and bring the distorted perovskite unit cell, which promotes the grain growth as observed in Fig.(3). The doping of Mn ions have the tendency to rearrange and aggregeat within limited space, leading to an increase in the size of particles and distortion of crystal [24].

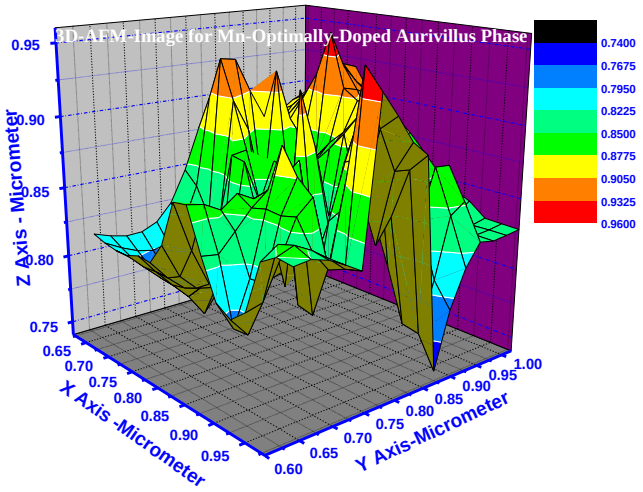

Fig.3c: 3D-image for Mn-212-BiSrV aurivillius with scanned zone 0.4x0.4x0.2 µm.

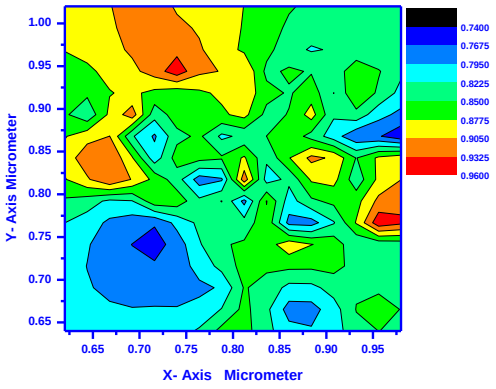

Fig.(3d): 2D-contour image for Mn-212-BiSrV aurivillius

with scanned zone 0.14x0.14 µm.

From Figs.3_b,3_c and 3_d one can observe the following facts that concluded from hyperfine 2 &3 dimension AFM investigations , surface of Mn-doped 212-BiSrV aurivillius is not smoothed and has a lot of heights gradient with minimum dark blue zones ~ 0.74 µm and maximum heights is for red-orange zones 0.96-1 µm .These heights gradient as appears in Fig.4 yields to maximum and huge surface area which qualifies Mn-doped aurivillius phase to play as superior surface catalyst .

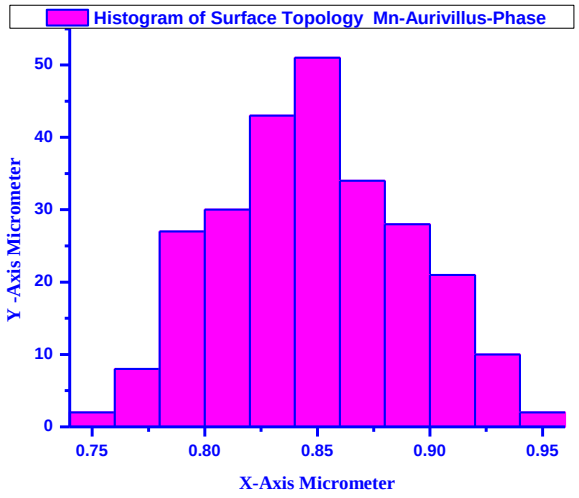

Fig.4: Histogram of Surface Topology for Mn-212-BiSrV aurivillius phase.

AFM-investigations confirmed that the grain size average of Mn-212-BiSrV is found to be (0.66-2.43 μm) which is nearly identical with those data mentioned in SEM (0.56-2.5 μm). This observation of particle size fitting is good evidence for structure homogeneity inside material bulk [23].

IV - Conclusions :

The conclusive remarks inside this article can summarize in the following points ;

1- Mn-substitution with optimum ratio x=0.1 mole are succeeded to replace V-sites on the $Bi_2SrV_{2-x}Mn_xO_9$ aurivillius structure without damaging hexagonal phase.

2- Mn-dopings interacted and affected sharply on IR-spectrum .

3- SEM and 3D-AFM investigations proved that Mn-optimally doped 212-BiSrV has huge surface area which qualifies Mn-doped aurivillius to play as superior surface catalyst in most common heterogeneous industrial processes.

References:

[1] K.Watanabe, m.Tanaka, E.Sumitomo, K.Katori, H.Yagi and J.F.Scott. Appl. Phys. Lett., 73, P.126,(1998).

[2] J.H.Yi, P.Thomas, M.Manier, J.P.Mercurio, I.Jauberteau and R.Guinebretiere, J.Sol-Gel Sci. Technol., 13, P.885, (1998).

[3] M.Mitsuya, K.Ishikawa, N.Nukaga and H.Funakubo, Jpn. J. Appl. Phys., part2, 39, P.L620, (2000).

[4] Y.Wu and $GBi_2SrV_{2-x}Zr_xO_9$.Z.Cao., J. Mater.Res. 15, P.1583, (2000).

[5] Y.Wu and G.Z.Cao., Appl. Phys. Lett., 75, P.2650, (1999).

[6] H.SGu, J.M.Xue and J.Wang, Appl. Phys. Lett.,79, P.2061, (2001).

[7] Y.Shimakawa, Y.Kubo, Y.Nakagawa, T.Kamiyama, H.Asano, F.Izumi, Appl. Phys. Lett., 74, P.1904, (1999).

[8] J.K.Lee, B.Park, K.S.Hong, J. Appl. Phys., 88, P.2825, (2000).

[9] Y.Shimakawa, Y.Kubo, Y.Nakagawa, T.Kamiyama, H.Asano, F.Izumi, Phys. Rev., B61, P.6559, (2000).

[10] I.Coondoo, A.K.Jha, S.K.Agarwal, Ceramics international, 33, P.41, (2007).

[11] R.D.Shannon, C.T.Prewitt, Acta Crystallogr., B25, P.925, (1969).

[12] H.Taguchi, A.Shimizu, M.Nagao, H.Kido, J.Ceram.Soc.Japan, 115, P.77, (2007).

[13] M.Matsuoka, Y.Matsuo, H.Sasaki, S.Hayagawa, J.Am.Ceram.Soc., P.108, (1972).

[14] H.Ueoka,Ferroelectrics, P.352, (1974).

[15] J.H.Choi, S.I.Lee, H.J.Sung, J.H.Park, S.M.Jhon, J.Colloid Interface Science, P.291, (2006).

[16] S.J.Liu, N.G.Fan, Chin.J.Chem.Phys., P.367, (2006).

[17] M.Li, M.Xu, H.Liang, X.Li, T.Xu, ActaPhys.-Chim.Sin., 24(8), P.1405, (2008).

[18] M.Ohtaki, H.Koga, T.Tokunaga, K.Eguchi, H.Arai, J.Solid State Chem., 120, P.105, (1995).

[19] B.Raveau, A.Maignan, C.Martin, M.hervieu, Mater.Res.Bull., 35, P.1579, (2001).

[20] D.Kuo, Y.Kao, Solid State Communications, 148, P.279, (2008).

[21] R.DShannon, Acta Cryst., A2, P.751, (1976).

[22] 39- N.Syam, K.B.Varma, Mater. Sci. and Eng., B90, P.246, (2002).

[23] Khaled M. Elsabawy , Morsy M. A. Sekkina, and Mohamed A. Asker, Solid State Sciences J.,12,2 (2010)pp.1094-1097 .

[24] 24-S.R.Kokare, S.A.Pawar, N.T.Padal and P.B.Joshi, Bull. Mater. Sci., 24(2), P.243, (2001).